

An Information-Theoretic Perspective on Successive Cancellation List Decoding and Polar Code Design

Mustafa Cemil Coşkun, *Student Member, IEEE*, Henry D. Pfister, *Senior Member, IEEE*

Abstract—This work identifies information-theoretic quantities that are closely related to the required list size for successive cancellation list (SCL) decoding to implement maximum-likelihood decoding. It also provides an approximation for these quantities that can be computed efficiently for very long codes. There is a concentration around the mean of the logarithm of the required list size for sufficiently large block lengths. We further provide a simple method to estimate the mean via density evolution for the binary erasure channel (BEC). Simulation results for the binary-input additive white Gaussian noise channel as well as the BEC demonstrate the accuracy of the mean estimate. A modified Reed-Muller code with dynamic frozen bits performs very close to the random coding union (RCU) bound down to the block error rate of 10^{-5} under SCL decoding with list size $L = 128$ when the block length is $N = 128$. The analysis shows how to modify the design to improve the performance when a more practical list size, e.g., $L = 32$, is adopted while keeping the performance with $L = 128$ unchanged. For the block length of $N = 512$, a design performing within 0.4 dB from the RCU bound down to the block error rate of 10^{-6} under an SCL decoder with list size $L = 1024$ is provided. The design is modified using the new guidelines so that the performance improves with practical list sizes, e.g., $L \in \{8, 32, 128\}$, outperforming 5G designs.

Index terms— Successive cancellation list decoding, Reed-Muller codes, polar codes, dynamic frozen bits, code design.

I. INTRODUCTION

Polar codes constitute the first deterministic construction of capacity-achieving codes for binary memoryless symmetric (BMS) channels with an efficient decoder [2]. While they achieve capacity under successive cancellation (SC) decoding, their initial performance was not competitive with low-density parity-check (LDPC) and Turbo codes. This changed with the advent of SC list (SCL) decoding and the addition of cyclic redundancy-check (CRC) outer codes [3]. Due to their competitive performance for short block lengths [4], they have

been adopted by the 5G standard [5]. Many authors have optimized polar codes and their variants to improve their performance for the SCL decoder [6]–[13].

An important property of the SCL decoder is that its performance matches the maximum-likelihood (ML) decoder if the list size is sufficiently large. In this work, we consider the theoretical question: “What list size suffices to achieve ML decoding performance for a given channel quality?”. Simulating SCL decoding with a large list size is infeasible for long codes and doesn’t provide much insight. Current works rely mostly on heuristics, e.g., see [7]–[9], [11], [13].

We identify information-theoretic quantities associated with the required list size and provide natural approximations that can be computed efficiently even for very long codes. Our analysis suggests new code design criteria for an SCL decoder with practical list sizes, e.g., $L \in \{8, 32, 128\}$ by modifying known codes, e.g., Reed-Muller (RM) codes [14], [15]. This is illustrated via example constructions for short- to moderate-length regime, e.g., $N \in \{128, 512\}$.

Using techniques similar to those for analyzing LDPC codes [16], [17], we show that the logarithm of required list size concentrates around the mean for large block lengths. For the binary erasure channel (BEC), we provide a simple Markov chain approximation to compute this mean using only density evolution and simulations show that it is quite accurate.

The paper is organized as follows. In Section II, we provide the preliminaries needed for the rest of the work. In Section III, we introduce the key quantities and use them to analyze the considered list decoders. The convergence properties are studied for general BMS channels as well as for the BEC in Section IV. Numerical results are presented in Section V for the binary-input additive white Gaussian noise channel (biAWGNC) and the BEC. Conclusions follow in Section VI.

II. BACKGROUND

Random variables (r.v.s) are denoted by upper case letters, e.g., X , and their realizations by the lower case counterparts, e.g., x . Random vectors are denoted by $X_i^j = (X_i, X_{i+1}, \dots, X_j)$ and their realizations by x_i^j . If $j < i$, then X_i^j is void. We use $[N]$ for the set $\{1, 2, \dots, N\}$. Subvectors with indices in $\mathcal{S} \subseteq [N]$ are denoted by $x_{\mathcal{S}} = (x_{i_1}, \dots, x_{i_{|\mathcal{S}|}})$ where $i_1 < \dots < i_{|\mathcal{S}|}$ enumerates the elements in \mathcal{S} with $|\mathcal{S}|$ being the cardinality of the set \mathcal{S} . We use $x_{\sim i}$ for the vector $x_{[N] \setminus \{i\}}$. Bold capital letters are used for matrices, e.g., \mathbf{X} .

Consider a BMS channel with binary input $X \in \{0, 1\}$ and general output $Y \in \mathcal{Y}$, i.e., $W : X \rightarrow Y$. The transition probabilities are given by $W(y|x) \triangleq \Pr(Y = y|X = x)$.

This paper was presented in part at the IEEE International Conference on Signal Processing and Communications, July 2020, Bangalore, India [1].

Mustafa Cemil Coşkun is with the Institute for Communications Engineering (LNT), Technical University of Munich, Munich, Germany (email: mustafa.coskun@tum.de). Parts of this work was carried out when he was also with the Institute of Communications and Navigation of the German Aerospace Center (DLR), Weßling, Germany and with the Department of Electrical and Computer Engineering, Duke University, Durham, USA.

Henry D. Pfister is with the Department of Electrical and Computer Engineering, Duke University, Durham, USA (email: henry.pfister@duke.edu).

The work of M. C. Coşkun was supported in part by the Helmholtz Gemeinschaft through the HGF-Allianz DLR@Uni project Munich Aerospace via the research grant “Efficient Coding and Modulation for Satellite Links with Severe Delay Constraints” and in part by the German Research Foundation (DFG) under Grant KR 3517/9-1. The work of H. D. Pfister was supported in part by the National Science Foundation under Grant No. 1718494. Any opinions, findings, conclusions, and recommendations expressed in this material are those of the authors and do not necessarily reflect the views of these sponsors.

A. Polar and Reed-Muller Codes

The polar transform of length $N = 2^n$ is denoted by $\mathbf{G}_N \triangleq \mathbf{G}_2^{\otimes n}$ which is the n -fold Kronecker product of the 2×2 binary Hadamard matrix

$$\mathbf{G}_2 \triangleq \begin{bmatrix} 1 & 0 \\ 1 & 1 \end{bmatrix}.$$

This is the key building block in Arıkan's polar codes [2] and RM codes [14], [15].

To define an (N, K) polar or RM code, one partitions the input vector into sub-vectors that carry information and frozen bits whose values are known by the receiver. The set of information and frozen indices are denoted, respectively, by $\mathcal{A} \subseteq [N]$ with $|\mathcal{A}| = K$, and $\mathcal{F} \triangleq [N] \setminus \mathcal{A}$. Thus, the input vector u_1^N can be split into information bits $u_{\mathcal{A}}$ and frozen bits $u_{\mathcal{F}}$. Then, the codeword $x = u\mathbf{G}_N$ is transmitted over the channel. This construction enables efficient SC decoding [2], [18]. For polar codes, the set \mathcal{A} is chosen to minimize a tight upper bound on the error probability under SC decoding; however, the set \mathcal{A} for an r -th order of length- N RM code, denoted by $\text{RM}(r, m)$, consists of the indices of rows in \mathbf{G}_N with the Hamming weight at least equal to 2^{m-r} .

B. Successive Cancellation Decoding

Let y_1^N be observations of the bits x_1^N through N copies of the BMS channel W . The SC decoder takes the following steps sequentially from $i = 1$ to $i = N$. If $i \in \mathcal{F}$, it sets \hat{u}_i to its frozen value. If $i \in \mathcal{A}$, it computes the soft estimate $p_i(\hat{u}_1^{i-1}) \triangleq \Pr(U_i = 1 | Y_1^N = y_1^N, U_1^{i-1} = \hat{u}_1^{i-1})$, and makes a hard decision accordingly as

$$\hat{u}_i = \begin{cases} 0 & \text{if } p_i(\hat{u}_1^{i-1}) < \frac{1}{2} \\ 1 & \text{otherwise.} \end{cases}$$

To understand the SC decoder, we focus on the effective channels seen by each of the input bits in u_1^N [2]. The SC decoder uses the entire y_1^N vector and all past decisions \hat{u}_1^{i-1} to generate the soft estimate $p_i(\hat{u}_1^{i-1})$ and the hard decision \hat{u}_i for u_i . Let $W_N^{(i)}$ denote the effective (virtual) channel seen by u_i during the SC decoding [2]. If all past bits u_1^{i-1} are provided by a genie, then this channel is easier to analyze. The effective channel $W_N^{(i)} : U_i \rightarrow (Y_1^N, U_1^{i-1})$ is then defined by its transition probabilities

$$W_N^{(i)}(y_1^N, u_1^{i-1} | u_i) \triangleq \sum_{u_{i+1}^N \in \{0,1\}^{N-i}} \frac{1}{2^{N-i}} W_N(y_1^N | u_1^N \mathbf{G}_N)$$

where $W_N(y_1^N | x_1^N) \triangleq \prod_{i=1}^N W(y_i | x_i)$.

C. Successive Cancellation List Decoding

SCL decoding of RM codes (and related subcodes) was introduced in [19]. These ideas were extended to optimized constructions of generalized concatenated codes in [18]. These approaches became popular after [3] applied them to polar codes that were combined with an outer CRC code to increase the minimum distance.

SCL decoding recursively computes $Q_i(\tilde{u}_1^i, y_1^N) \propto \Pr(U_1^i = \tilde{u}_1^i, Y_1^N = y_1^N)$ for $i = 1, \dots, N$ via the SC message

passing rules for partial input sequences $\tilde{u}_1^i \in \mathcal{U}_i \subseteq \{0,1\}^i$. Discarding y_1^N for the ease of notation, we refer to $Q_i(\tilde{u}_1^i)$ as the *myopic likelihood* of the sequence \tilde{u}_1^i as it does not use the receiver's knowledge of frozen bits after u_i .

Let $\mathcal{U}_{i-1} \subseteq \{0,1\}^{i-1}$ be a subset satisfying $|\mathcal{U}_{i-1}| = L$ and assume that $Q_{i-1}(\tilde{u}_1^{i-1})$ is known for some $\tilde{u}_1^{i-1} \in \mathcal{U}_{i-1}$. Then, for $\tilde{u}_i \in \{0,1\}$, one can write

$$Q_i(\tilde{u}_1^i) \propto \Pr(U_1^i = \tilde{u}_1^i, Y_1^N = y_1^N) \\ \propto Q_{i-1}(\tilde{u}_1^{i-1}) \Pr(U_i = \tilde{u}_i | Y_1^N = y_1^N, U_1^{i-1} = \tilde{u}_1^{i-1}) \quad (1)$$

where the right-most term can be computed efficiently by the SC decoder starting from $Q_0(\tilde{u}_1^0) \triangleq 1$. This results in $Q_i(\tilde{u}_1^i)$ values for $2L$ partial sequences. One then prunes the list down to L sequences by keeping only most likely paths according to (1) for an SCL decoder with list size L . Note that if u_i is frozen, then the decoder simply extends all paths with correct frozen bit. After the N -th decoding stage, the estimate \hat{u}_1^N is chosen as the candidate maximizing the function $Q_N(\tilde{u}_1^N)$.

For the BEC, all partial input sequences $u_1^i \in \{0,1\}^i$ with $Q_i(u_1^i) > 0$ are equiprobable. Hence, for a given u_1^{i-1} , we have $p_i(u_1^{i-1}) \in \{0, \frac{1}{2}, 1\}$. If $p_i(u_1^{i-1}) \in \{0,1\}$, then u_i is known perfectly at the receiver. However, if $p_i(u_1^{i-1}) = \frac{1}{2}$ and u_i is not frozen, then \hat{u}_i can be seen as an erasure. When an information bit is decoded to an erasure, it is replaced by both possible values (assuming the list size is large enough) and decoding proceeds separately under these two hypotheses. The number of hypotheses (i.e., partial input sequences) is halved if the decoded value for a frozen bit contradicts with its actual value [20, Appendix A]. An error is declared if, at any decoding stage, the number of hypotheses exceeds L or if there are more than one hypothesis at the process, i.e., if $\exists \tilde{u}_1^N \in \{0,1\}^N$, $\tilde{u}_1^N \neq u_1^N$ with $Q_N(\tilde{u}_1^N) > 0$.

D. Successive Cancellation Inactivation Decoding

SC inactivation (SCI) decoding is a more efficient version of SCL decoding for the BEC proposed in [21]. It follows the same decoding schedule as the SCL decoder but instead replaces an erased information bit by an unknown variable, i.e., the bit is *inactivated* [22]–[24]. Later, some inactivated bits may be resolved using linear equations derived from decoding frozen bits. This can be done at each stage of the decoding process or delayed until the end. When dummy variables are eliminated without delaying to the end of decoding, we refer to this as a *consolidation* event. In this work, our focus is on the SCI decoder with consolidations.

During SCI decoding, if $p_i(u_1^{i-1}) = \frac{1}{2}$ and u_i is not frozen, then u_i is inactivated by introducing a dummy variable \tilde{u}_i and storing the decision as $\hat{u}_i = \tilde{u}_i$. It continues decoding using SC decoding for the BEC except that the message values are allowed to be a function of all inactivated variables. Finally, the inactivated bits are typically resolved using linear equations derived from decoding frozen bits.

The SCI decoder can inactivate multiple bits if required. If the maximum number of inactivations is not bounded, then it implements ML decoding. For further details, see [21].

E. Dynamic Frozen Bits

An important observation in [6] is that decoders having the successive nature (e.g., SCL or SCI decoders) still work (with slight modifications) if, for some $i \in \mathcal{F}$, the bit u_i is a function of a set of preceding information bits. A frozen bit whose value depends on past inputs is called dynamic.

A polar code with dynamic frozen bits is defined by its information indices \mathcal{A} and a matrix that defines each frozen bit as a linear combination of preceding information bits. There are now a number of approaches for choosing these parameters [6], [7] and heuristic design methods [8], [13]. In this work, after specifying \mathcal{A} , we define each frozen bit to be a uniform random linear combination of information bits preceding it.

III. ANALYSIS OF THE LIST DECODERS

An important property of list decoding is that, if the correct codeword is on the list at the end of decoding, then the error probability is upper bounded by that of the ML decoder. We study how large the list should be at each stage so that the correct codeword is likely to be on the list.

A. An Information-Theoretic Perspective

Consider a length- N polar code with SCL decoding after the m -th decoding stage. Since SCL decoding does not use future frozen bits, we focus on the subset of length- m input patterns that have significant conditional entropy given the channel observation. An important insight is that, after observing Y_1^N , the uncertainty in U_1^m is quantified by the entropy

$$H(U_1^m | Y_1^N) = \sum_{i=1}^m H(U_i | U_1^{i-1}, Y_1^N) \quad (2)$$

where U_1^N is assumed to be uniform over $\{0, 1\}^N$. This is exactly true if the first m bits are all information bits, i.e., if $[m] \subseteq \mathcal{A}$. If $[m]$ contains also frozen indices, however, then the situation is more complicated.

Let $\mathcal{A}^{(m)} \triangleq \mathcal{A} \cap [m]$ and $\mathcal{F}^{(m)} \triangleq \mathcal{F} \cap [m]$ be the sets containing information and frozen indices within the first m input bits, respectively. Now consider an experiment where the frozen bits U_i with $i \in \mathcal{F}^{(m)}$ are uniform and independent of U_1^{i-1} . Using (2) naively with the assumption that $U_{\mathcal{F}^{(m)}}$ is not known to the receiver would cause an overestimate of $H(U_1^m | Y_1^N)$ by an amount of at least $\sum_{i \in \mathcal{F}^{(m)}} H(U_i | U_1^{i-1}, Y_1^N)$. In addition to this, the frozen bits $U_{\mathcal{F}^{(m)}}$ may reveal additional information about the previous information bits.

To better understand the uncertainty within the first m input bits during SCL decoding, we define the quantities

$$d_m \triangleq H(U_{\mathcal{A}^{(m)}} | Y_1^N, U_{\mathcal{F}^{(m)}}) \quad \text{and} \quad \Delta_m \triangleq d_m - d_{m-1}.$$

Observe that, if U_m is an information bit, then we have

$$\begin{aligned} \Delta_m &= H(U_{\mathcal{A}^{(m)}} | Y_1^N, U_{\mathcal{F}^{(m)}}) - H(U_{\mathcal{A}^{(m-1)}} | Y_1^N, U_{\mathcal{F}^{(m-1)}}) \\ &= H(U_{\mathcal{A}^{(m)}} | Y_1^N, U_{\mathcal{F}^{(m-1)}}) - H(U_{\mathcal{A}^{(m-1)}} | Y_1^N, U_{\mathcal{F}^{(m-1)}}) \\ &= H(U_{\mathcal{A}^{(m)}}, U_{\mathcal{F}^{(m-1)}} | Y_1^N) - H(U_{\mathcal{A}^{(m-1)}}, U_{\mathcal{F}^{(m-1)}} | Y_1^N) \\ &= H(U_1^{m-1} | Y_1^N) + H(U_m | Y_1^N, U_1^{m-1}) - H(U_1^{m-1} | Y_1^N) \\ &= H(U_m | Y_1^N, U_1^{m-1}) \end{aligned} \quad (3)$$

which is exactly what one would expect from the naive analysis given by (2).

If U_m is a frozen bit, then consider a model where it is not known to the receiver at the time of transmission.¹ The act of revealing U_m to the receiver changes the conditional uncertainty about $U_{\mathcal{A}^{(m-1)}}$ by

$$\begin{aligned} \Delta_m &= H(U_{\mathcal{A}^{(m)}} | Y_1^N, U_{\mathcal{F}^{(m)}}) - H(U_{\mathcal{A}^{(m-1)}} | Y_1^N, U_{\mathcal{F}^{(m-1)}}) \\ &= H(U_{\mathcal{A}^{(m-1)}} | Y_1^N, U_{\mathcal{F}^{(m-1)}}, U_m) - H(U_{\mathcal{A}^{(m-1)}} | Y_1^N, U_{\mathcal{F}^{(m-1)}}) \\ &= -I(U_m; U_{\mathcal{A}^{(m-1)}} | Y_1^N, U_{\mathcal{F}^{(m-1)}}) \\ &= H(U_m | Y_1^N, U_1^{m-1}) - H(U_m | Y_1^N, U_{\mathcal{F}^{(m-1)}}) \\ &\geq H(U_m | Y_1^N, U_1^{m-1}) - 1. \end{aligned} \quad (4)$$

This expression quantifies the effect of revealing the new frozen bit as a reduction in the conditional entropy of the information bits preceding it. A large reduction may occur when the channel $W_N^{(m)}$ has low entropy (i.e., a low-entropy effective channel is essentially frozen) and the reduction will be small if the channel entropy is high (i.e., the input is unpredictable from Y_1^N and U_1^{m-1}).

For BMS channels, we can combine (3) and (4) to understand the dynamics of d_m . This gives a proxy for the uncertainty in the SCL decoding after m steps. We have

$$\sum_{i \in \mathcal{A}^{(m)}} H(W_N^{(i)}) - \sum_{i \in \mathcal{F}^{(m)}} (1 - H(W_N^{(i)})) \leq d_m \quad (5a)$$

$$\leq \sum_{i \in \mathcal{A}^{(m)}} H(W_N^{(i)}) \quad (5b)$$

The lower bound assumes that frozen bits (when perfectly observed) always reduce the entropy.

Theorem 1. Upon observing y_1^N when u_1^N is transmitted, the set of partial sequences \tilde{u}_1^m with a larger likelihood than some fraction, determined by a positive number $\alpha \leq 1$, of that for true sequence u_1^m after m stages of SCL decoding is given by $\mathcal{S}_\alpha^{(m)}(u_1^m, y_1^N) \triangleq \{\tilde{u}_1^m : Q_m(\tilde{u}_1^m) \geq \alpha Q_m(u_1^m)\}$. On average, the logarithm of its cardinality is upper bounded by

$$\begin{aligned} \mathbb{E}[\log_2 |\mathcal{S}_\alpha^{(m)}|] &\leq d_m + \log_2 \alpha^{-1} \\ &= H(U_{\mathcal{A}^{(m)}} | Y_1^N, U_{\mathcal{F}^{(m)}}) + \log_2 \alpha^{-1}. \end{aligned} \quad (6)$$

Proof. Assume, w.l.o.g., that u_1^N and y_1^N are transmitted and observed, respectively. Then, we have

$$\begin{aligned} \log_2 |\mathcal{S}_\alpha^{(m)}| &\stackrel{(a)}{=} \log_2 \sum_{\tilde{u}_1^m} \mathbb{1}_{(p(\tilde{u}_{\mathcal{A}^{(m)}} | y_1^N, u_{\mathcal{F}^{(m)}}) \geq \alpha \cdot p(u_{\mathcal{A}^{(m)}} | y_1^N, u_{\mathcal{F}^{(m)}}))} \\ &\stackrel{(b)}{\leq} -\log_2 \alpha \cdot p(u_{\mathcal{A}^{(m)}} | y_1^N, u_{\mathcal{F}^{(m)}}) \end{aligned}$$

where (a) follows from $Q_m(u_1^m) \propto \Pr(U_1^m = \tilde{u}_1^m, Y_1^N = y_1^N)$ and Bayes' rule and (b) from the fact that if there are more than $(\alpha \cdot p(u_{\mathcal{A}^{(m)}} | y_1^N, u_{\mathcal{F}^{(m)}}))^{-1}$ sequences $\tilde{u}_{\mathcal{A}}$ with probability $\alpha \cdot p(u_{\mathcal{A}^{(m)}} | y_1^N, u_{\mathcal{F}^{(m)}})$, then the total probability exceeds 1.

¹This reflects how the SCL decoder operates, i.e., it does not use the knowledge of any frozen bit U_m until reaching the end of its decoding stage m . The soft estimate $p_m(u_1^{m-1})$ provides an additional information to separate the hypotheses (i.e., paths) although the hard estimate is chosen as $\hat{u}_m = u_m$ independent of $p_m(u_1^{m-1})$.

As the inequality is valid for any pair u_1^N and y_1^N , taking the expectation over all u_1^m and y_1^N yields the stated result. \square

Now, consider an SCL decoder whose list size is L_m during the m -th decoding step. Then, the decoder should satisfy $L_m \geq |\mathcal{S}_1^{(m)}|$ for the true u_1^m to be in the set $\mathcal{S}_1^{(m)}$. Using (6) and (5b) yields the simple upper bound

$$\mathbb{E} \left[\log_2 |\mathcal{S}_1^{(m)}| \right] \leq \sum_{i \in \mathcal{A}^{(m)}} H \left(W_N^{(i)} \right) + \log_2 \alpha^{-1}. \quad (7)$$

Remark 1. The analysis in terms of $\log_2 L_m$ has two weaknesses. First, the entropy d_m only characterizes typical events, e.g., ensuring that the correct codeword stays on the list at least half of the time, whereas coding typically focuses on rarer events, e.g., block error rates less than 10^{-2} . Second, the sequence d_m is averaged over Y_1^N but the actual decoder sees a random realization $d_m(y_1^N) = H(U_{\mathcal{A}^{(m)}} | Y_1^N = y_1^N, U_{\mathcal{F}^{(m)}})$. Nevertheless, we believe the results provide a useful step towards a theoretical analysis of the SCL decoder. The numerical results in Section V illustrate the accuracy of the analysis. To motivate the analysis further, we study the convergence properties of the r.v. $D_m \triangleq d_m(Y_1^N)$ in Section IV.²

Remark 2. The results have significance for code design. To achieve good performance with an SCL decoder whose list size is L_m during the m -th decoding step, a reasonable first-order design criterion is that $\log_2 L_m \geq d_m$. This observation implies, in principle, that frozen bits should be allocated to prevent d_m from exceeding $\log_2 L_m$. Exemplary designs are provided in Section V-A.

B. The Binary Erasure Channel

Proposition 1. On the BEC, the list of all valid partial information sequences $u_{\mathcal{A}^{(m)}}$ generated by SCL decoding with unbounded list size form an affine subspace.

Proof. Let \mathcal{E} denote the set of erased positions in the realization y_1^N . Then, we can write

$$(u_{\mathcal{A}^{(m)}}, u_{m+1}^N) \mathbf{G}'_{[N] \setminus \mathcal{F}^{(m)}} = y_{[N] \setminus \mathcal{E}} \oplus u_{\mathcal{F}^{(m)}} \mathbf{G}'_{\mathcal{F}^{(m)}} \quad (8)$$

where $\mathbf{G}'_{\mathcal{S}}$ is the matrix formed by the rows of \mathbf{G}_N indexed in \mathcal{S} and then removing its columns indexed in \mathcal{E} and \oplus is the bit-wise XOR of two vectors. This equation enables to use the frozen bits $u_{\mathcal{F}^{(m)}}$ as side information. Let \mathcal{C} denote the set of all possible solutions for $(u_{\mathcal{A}^{(m)}}, u_{m+1}^N)$, which is an affine subspace. We are interested in all compatible partial information sequences $u_{\mathcal{A}^{(m)}}$ with (8) (hence, u_1^m as $u_{\mathcal{F}^{(m)}}$ is a linear transform of $u_{\mathcal{A}^{(m)}}$). To this end, we define the mapping $\Pi_{\mathcal{A}^{(m)}} : \mathbb{F}_2^{N-|\mathcal{F}^{(m)}|} \rightarrow \mathbb{F}_2^{|\mathcal{A}^{(m)}|}$ as

$$\Pi_{\mathcal{A}^{(m)}}(\mathcal{C}) \triangleq \left\{ v_1^{|\mathcal{A}^{(m)}|} : v_1^{N-|\mathcal{F}^{(m)}|} \in \mathcal{C} \right\}$$

which is a linear mapping since it can be represented as a multiplication of the input by a matrix formed by stacking an $|\mathcal{A}^{(m)}| \times |\mathcal{A}^{(m)}|$ identity matrix and an $(N-m) \times |\mathcal{A}^{(m)}|$ all-zero matrix. Then, the result follows by noting that a linear transform of an affine subspace is affine. \square

²Note the difference between the definitions d_m , $d_m(y_1^N)$ and $d_m(Y_1^N)$, which should be used carefully.

For the BEC, the SCI decoder provides a concrete example of the information-theoretic perspective. As shown in Proposition 1, the set of valid information sequences after m decoding steps is an affine subspace of $\{0, 1\}^{|\mathcal{A}^{(m)}|}$. SCI decoding stores a basis for this vector subspace instead of listing all possible sequences in it. For any y_1^N , the subspace dimension is $d_m(y_1^N) = H(U_{\mathcal{A}^{(m)}} | Y_1^N = y_1^N, U_{\mathcal{F}^{(m)}})$.

Let $\epsilon_N^{(m)} \triangleq \Pr(p_i(u_1^{i-1}) = \frac{1}{2})$, where the implied randomness is due to the received vector. Consider the decoding of information and frozen bits given the observed vector and preceding frozen bits. When an information bit u_m is decoded, one of following events occurs:

- The information bit is decoded as an erasure and the subspace dimension increases by one, i.e., $d_m(y_1^N) = d_{m-1}(y_1^N) + 1$. Averaged over all y_1^N , the probability of this event equals $\epsilon_N^{(m)}$ [21].
- The information bit is decoded as an affine function of the previous information bits and the subspace dimension is unchanged, i.e., $d_m(y_1^N) = d_{m-1}(y_1^N)$. Averaged over all y_1^N , the probability of this event equals $1 - \epsilon_N^{(m)}$ [21].

If a frozen u_m is decoded, one of following events occurs:

- The decoder returns an erasure for the frozen bit. In this case, revealing the true value of the frozen bit allows decoding to continue, but no new information is provided about preceding information bits. Thus, we have $d_m(y_1^N) = d_{m-1}(y_1^N)$. Averaged over all y_1^N , the probability of this event equals $1 - \epsilon_N^{(m)}$ [21].
- The frozen bit is decoded as an affine function of the previous information bits. Averaged over all y_1^N , the probability of this event equals $1 - \epsilon_N^{(m)}$ [21]. In this case, revealing the true value of the frozen bit gives a linear equation for a subset of the preceding information bits. If the linear equation is informative, then the subspace dimension decreases by one via a consolidation event, i.e., we have $d_m(y_1^N) = d_{m-1}(y_1^N) - 1$. Otherwise, the dimension is unchanged, i.e., $d_m(y_1^N) = d_{m-1}(y_1^N)$.

At first glance, these rules might appear to tell the whole story. But the erasure rate $\epsilon_N^{(m)}$ is averaged over all y_1^N whereas predicting the value of D_m requires the conditional probability of erasure events given all past observations. More importantly, to understand consolidation events, one needs to compute the probability that the obtained equation is informative.

Since we do not have expressions for these quantities,³ we use two simplifying approximations. First, we approximate the probability of decoding an erasure for a frozen bit as independent of all past events. Second, we approximate the probability that an informative equation obtained from consolidation by $1 - 2^{-D_{m-1}}$, independent of past events. This value comes from modeling the obtained equation and the subset using a uniform random model. Under these assumptions, the random sequence D_1, \dots, D_N can be approximated by an inhomogeneous Markov chain with transition probabilities

³Even if we had them exactly, they may be too complicated to be useful.

$P_{i,j}^{(m)} \approx \Pr(D_m = j \mid D_{m-1} = i)$ where

$$P_{i,j}^{(m)} = \begin{cases} \epsilon_N^{(m)} & \text{if } m \in \mathcal{A}, j = i + 1 \\ 1 - \epsilon_N^{(m)} & \text{if } m \in \mathcal{A}, j = i \\ \epsilon_N^{(m)} + (1 - \epsilon_N^{(m)}) 2^{-D_{m-1}} & \text{if } m \in \mathcal{F}, j = i \\ (1 - \epsilon_N^{(m)}) (1 - 2^{-D_{m-1}}) & \text{if } m \in \mathcal{F}, j = i - 1. \end{cases} \quad (9)$$

Based on this Markov chain approximation, one can make a further approximation by computing the expectation $d_m = \mathbb{E}[D_m]$ and approximating $\mathbb{E}[2^{-D_m}] \approx 2^{-d_m}$. By setting $d_0 \triangleq 0$, this gives the simple recursive approximation

$$d_m \approx \begin{cases} d_{m-1} + \epsilon_N^{(m)} & \text{if } m \in \mathcal{A} \\ \left[d_{m-1} - (1 - 2^{-d_{m-1}}) (1 - \epsilon_N^{(m)}) \right]^+ & \text{if } m \in \mathcal{F} \end{cases} \quad (10)$$

where $[\cdot]^+ \triangleq \max\{0, \cdot\}$.

IV. CONCENTRATION FOR LIST DECODERS

This section studies the stochastic convergence properties of the r.v. D_m . In particular, we show that the required uncertainty accumulated by an SCL decoder to keep the correct path on the list concentrates around its mean d_m for sufficiently large block lengths.

A. General Approach

We form a Doob's Martingale by sequentially revealing information about the object of interest (e.g., see [16], [17]), which is the conditional entropy in our case. In N consecutive steps, we reveal the random channel realizations. Irrespective of the revealed realization, the change in the subspace dimension is bounded by some constant. This lets us use the Azuma-Hoeffding inequality [25, Thm. 12.6] since the channels under consideration are memoryless.

Proposition 2. *The sequence of r.v.s $H_0^{(m)}, H_1^{(m)}, \dots, H_N^{(m)}$ where $H_i^{(m)} \triangleq \mathbb{E}[D_m | Y_1^i]$ is a Doob's Martingale, i.e.,*

$$H_i^{(m)} \text{ is a function of } Y_1^i \quad (11)$$

$$\mathbb{E}[|D_m|] < \infty \quad (12)$$

$$H_{i-1}^{(m)} = \mathbb{E}[H_i^{(m)} | Y_1^{i-1}]. \quad (13)$$

Proof. The statement (11) follows from the construction of r.v.s $H_i^{(m)}$ and the definition of conditional expectation. The inequality (12) follows from the non-negativity of D_m and $\mathbb{E}[D_m] = H(U_{\mathcal{A}^{(m)}} | Y_1^N, U_{\mathcal{F}^{(m)}})$. Finally, (13) follows by

$$\mathbb{E}[H_i^{(m)} | Y_1^{i-1}] = \mathbb{E}[\mathbb{E}[D_m | Y_1^i] | Y_1^{i-1}] \quad (14)$$

$$= \mathbb{E}[D_m | Y_1^{i-1}] \quad (15)$$

$$= H_{i-1}^{(m)} \quad (16)$$

where (14) and (16) follow from the definition of $H_i^{(m)}$, and (15) from the tower property [26, Eq. (C.13)]. \square

Proposition 3. *Consider transmission over a BMS channel satisfying $W(y|x) \geq \delta > 0, \forall y \in \mathcal{Y}, \forall x \in \{0, 1\}$. Then, for*

all $i \in [N]$ and all values y_1^N and \tilde{y}_1^N such that $y_{\sim i} = \tilde{y}_{\sim i}$ and $y_i \neq \tilde{y}_i$, the conditional entropy satisfies

$$|d_m(y_1^N) - d_m(\tilde{y}_1^N)| \leq 4 |\log_2 \delta|. \quad (17)$$

Proof. In the following, the r.v.s are not explicitly written in the probability assignments, e.g., the probabilities are denoted as $p(u_1^m, x_1^N, y_1^N) = \Pr(U_1^m = u_1^m, X_1^N = x_1^N, Y_1^N = y_1^N)$.

The proof starts by writing

$$\begin{aligned} \frac{p(u_{\mathcal{A}^{(m)}} | y_1^N, u_{\mathcal{F}^{(m)}})}{p(u_{\mathcal{A}^{(m)}} | \tilde{y}_1^N, u_{\mathcal{F}^{(m)}})} &\stackrel{(a)}{=} \frac{p(u_1^m, y_1^N)}{p(y_1^N, u_{\mathcal{F}^{(m)}})} \cdot \frac{p(\tilde{y}_1^N, u_{\mathcal{F}^{(m)}})}{p(u_1^m, \tilde{y}_1^N)} \\ &\stackrel{(b)}{=} \frac{\sum_{x_1^N} p(u_1^m, x_1^N, y_1^N)}{\sum_{x_1^N} p(y_1^N, x_1^N, u_{\mathcal{F}^{(m)}})} \cdot \frac{\sum_{x_1^N} p(\tilde{y}_1^N, x_1^N, u_{\mathcal{F}^{(m)}})}{\sum_{x_1^N} p(u_1^m, x_1^N, \tilde{y}_1^N)} \\ &\stackrel{(c)}{=} \frac{\sum_{x_i} W(y_i | x_i) \sum_{x_{\sim i}} p(u_1^m, x_1^N, y_{\sim i})}{\sum_{x_i} W(\tilde{y}_i | x_i) \sum_{x_{\sim i}} p(u_1^m, x_1^N, y_{\sim i})} \\ &\quad \cdot \frac{\sum_{x_i} W(\tilde{y}_i | x_i) \sum_{x_{\sim i}} p(y_{\sim i}, x_1^N, u_{\mathcal{F}^{(m)}})}{\sum_{x_i} W(y_i | x_i) \sum_{x_{\sim i}} p(y_{\sim i}, x_1^N, u_{\mathcal{F}^{(m)}})} \\ &\stackrel{(d)}{=} \frac{\sum_{x_i} W(y_i | x_i) p(u_1^m, x_i, y_{\sim i})}{\sum_{x_i} W(\tilde{y}_i | x_i) p(u_1^m, x_i, y_{\sim i})} \\ &\quad \cdot \frac{\sum_{x_i} W(\tilde{y}_i | x_i) p(y_{\sim i}, x_i, u_{\mathcal{F}^{(m)}})}{\sum_{x_i} W(y_i | x_i) p(y_{\sim i}, x_i, u_{\mathcal{F}^{(m)}})} \end{aligned} \quad (18)$$

where (a) follows from Bayes' rule, (b) and (d) from the law of total probability, and (c) from rearranging the summation, Bayes' rule and noting that $Y_i - X_i - (U_1^m, X_{\sim i}, Y_{\sim i})$ forms a Markov chain. Then, we take the logarithm and absolute value of both sides in (18). Combining the triangle inequality, i.e., $|a + b| \leq |a| + |b|$, with the fact that each summand is upper bounded by $\max_y |\log_2 W(y|0)|$, e.g.,

$$\left| \log_2 \sum_{x_i} W(y_i | x_i) p(u_1^m, x_i, y_{\sim i}) \right| \leq \max_y |\log_2 W(y|0)|$$

we conclude that

$$\left| \log_2 \frac{p(u_{\mathcal{A}^{(m)}} | y_1^N, u_{\mathcal{F}^{(m)}})}{p(u_{\mathcal{A}^{(m)}} | \tilde{y}_1^N, u_{\mathcal{F}^{(m)}})} \right| \leq 4 \max_y |\log_2 W(y|0)|. \quad (19)$$

Since (19) is valid for any u_1^m , averaging over all u_1^m , combined with the Jensen's inequality, leads to (17) by noting $W(y|0) \geq \delta, \forall y \in \mathcal{Y}$. \square

As a result of Proposition 3, the following corollary provides a concentration for the logarithm of the list size required to approach the performance of a code under ML decoding when the transmission is over discrete output BMS channels. More precisely, the normalized (with respect to the block length) deviation of the logarithm of the random list size, required to keep the correct codeword in the list, from the average decays exponentially fast.

Corollary 1. *For transmission over a BMS channel satisfying $W(y|x) \geq \delta > 0, \forall y \in \mathcal{Y}, \forall x \in \{0, 1\}$, the r.v. $D_m, m \in [N]$, for a particular random realization Y_1^N concentrates around its mean d_m for sufficiently large block lengths, i.e., for any $\beta > 0$, we have*

$$\Pr \left\{ \frac{1}{N} |D_m - d_m| > \beta \right\} \leq 2 \exp \left(- \frac{\beta^2}{8 |\log_2 \delta|} N \right).$$

Proof. Apply the Azuma-Hoeffding inequality [25, Thm. 12.6] via Proposition 3 since the channel is memoryless. \square

Since $\delta = 0$ for the BEC, it will be considered separately in the next section. For the case where $W(y|0)$ is a continuous probability density function on a compact set $\mathcal{Y} \subset \mathbb{R}$, the same proof applies with $\delta = \min_{y \in \mathcal{Y}} W(y|0)$. But, the proof does not extend to unbounded output alphabets.

B. The Binary Erasure Channel

SCI decoding over the BEC is equivalent to solving a system of linear equations with side information depending on the decoding stage. In other words, the decoder has the knowledge of the frozen bits $u_{\mathcal{F}^{(m)}}$ after the decoding stage m as side information.

Proposition 4. *For transmission over the BEC, the subspace dimension satisfies the Lipschitz-1 condition: for all $i \in [N]$ and all values y_1^N and \tilde{y}_1^N such that $y_{\sim i} = \tilde{y}_{\sim i}$ and $y_i \neq \tilde{y}_i$, the subspace dimension satisfies*

$$|d_m(y_1^N) - d_m(\tilde{y}_1^N)| \leq 1. \quad (20)$$

Proof. It suffices to consider the case where y_i is not erased, but \tilde{y}_i is an erasure (i.e., $y_i = x_i$ and $\tilde{y}_i = ?$). Recall the linear system given as (8). All compatible vectors $(u_{\mathcal{A}^{(m)}}, u_{m+1}^N)$, $m \in [N]$, with (8) form an affine subspace. The dimension of this subspace is equal to $d'_N(y_1^N) = n - |\mathcal{F}^{(m)}| - \text{rank}(\mathbf{G}'_N)$. Since removing one more column of \mathbf{G}'_N (and also of $\mathbf{G}'_{\mathcal{F}^{(m)}}$) cannot decrease the rank by more than one, we have

$$d'_N(y_1^N) \leq d'_N(\tilde{y}_1^N) \leq d'_N(y_1^N) + 1. \quad (21)$$

Hence, the number of compatible vectors $(u_{\mathcal{A}^{(m)}}, u_{m+1}^N)$ with (8) is (at most) doubled or unchanged.

We are interested in the subspace dimension $d_m(y_1^N)$. This is equal to the number of different subvectors $u_{\mathcal{A}^{(m)}}$ of all compatible $(u_{\mathcal{A}^{(m)}}, u_{m+1}^N)$ with (8). Using (21), one concludes that the number of different vectors $u_{\mathcal{A}^{(m)}}$ either increases by a factor of 2 or does not change, resulting in (20). \square

Corollary 2. *The subspace dimension D_m for a particular random realization Y_1^N concentrates around its mean d_m for sufficiently large block lengths, i.e., for any $\beta > 0$, we have*

$$\Pr \left\{ \frac{1}{N} |D_m - d_m| > \beta \right\} \leq 2 \exp \left(-\frac{\beta^2}{2} N \right). \quad (22)$$

Proof. As for Corollary 1, apply the Azuma-Hoeffding inequality [25, Thm. 12.6] via Proposition 4. \square

Remark 3. *Let $\rho = \lceil \log_2 m \rceil$ and $N_0 = 2^\rho$. Due to the recursive structure of the SCL decoder, the statistics of D_m are the same for all $N \geq N_0$ if the first N_0 frozen bits are the same. Thus, Corollary 2 remains valid if we replace (22) by*

$$\Pr \left\{ \frac{1}{N_0} |D_m - d_m| > \beta \right\} \leq 2 \exp \left(-\frac{\beta^2}{2} N_0 \right).$$

This provides a significant improvement when $N_0 \ll N$. The same idea can also be applied to Corollary 1 but the value of δ must be modified as well.

V. SIMULATION RESULTS

This section provides simulation results are provided for some constructions with dynamic frozen bits. In particular, we consider instances from an ensemble of modified RM codes, namely d-RM codes [21].

Definition 1. *The d-RM(r, m) ensemble, denoted by $\mathcal{C}(r, m)$, is the set of all codes, specified by set \mathcal{A} of the RM(r, m) code and setting, for $i \in \mathcal{F}$,*

$$u_i = \begin{cases} \sum_{j \in \mathcal{A}^{(i-1)}} v_{j,i} u_j & \text{if } \mathcal{A}^{(i-1)} \neq \emptyset \\ 0 & \text{otherwise.} \end{cases}$$

with all possible $v_{j,i} \in \{0, 1\}$ and $\mathcal{A}^{(0)} \triangleq \emptyset$.

Recently, Arıkan introduced polarization-adjusted convolutional (PAC) codes [12], which can be represented as a polar code with dynamic frozen bits [27], [28]. The rate-profiling choice of a PAC code is directly reflected in the frozen index set of its polar code representation [27]. Thus, if \mathcal{A} of an RM(r, m) code is chosen as the rate-profiling (as in [12]), then the corresponding PAC code becomes an instance from $\mathcal{C}(r, m)$. Another instance is the RM(r, m) code.

A. The Binary-Input Additive White Gaussian Channel

Fig. 1 shows simulation results for a random instance from $\mathcal{C}(3, 7)$ and a novel design (based on suggestions in Remark 2) under SCL decoding with $L = 2^{14}$ and $E_b/N_0 = 0.5$ together with the upper and lower bounds (5b) and (5a) on d_m . The proposed code takes the set \mathcal{A}_{RM} of the (128, 64) RM code and obtains a new set as $\mathcal{A} = (\mathcal{A}_{\text{RM}} \setminus \{30, 40\}) \cup \{1, 57\}$, i.e., $u_{\{30, 40\}}$ are frozen and $u_{\{1, 57\}}$ are unfrozen, where each frozen bit is still set to a random linear combination of preceding information bit(s). This helps especially for the considered list size $L = 32$. The reason is illustrated by the lower bounds on d_m in Fig. 1. In addition to having a smaller peak value, this peak occurs for the proposed design later than for the d-RM code. This helps for the proposed code to keep the correct path in the list towards the end for small list sizes, e.g., $L = 32$. If the list size is further decreased, then having u_1 as information bit can cause a degradation. Notice that there is no visible degradation in the ML performance. Fig. 1 validates the bounds (5a), (5b) and (7). Note that we set the parameter $\alpha = 0.94$ in (6) to provide a robust estimate by capturing the near misses. Also, (7) is tight for the entire range and (5a) closely tracks the simulation for $m \leq 50$.

Fig. 2 compares the performance of the d-RM and proposed codes. When an SCL decoder with $L = 128$ is considered, both codes perform within 0.15 dB of the random coding union (RCU) bound [29, Thm. 16] at a block error rate of 10^{-5} and they almost match the simulation-based ML lower bounds [3], denoted as ML LB in the figure. When a smaller list size, e.g., $L = 32$, is adopted, the proposed code outperforms the d-RM code especially at higher SNR values. This validates the analysis illustrated in Fig. 1. The performance for the 5G design under SCL decoding with $L = 32$ [30] is 0.4 dB worse than the proposed design at a block error rate around 10^{-4} . The metaconverse (MC) bound [29, Thm. 28] is also provided.

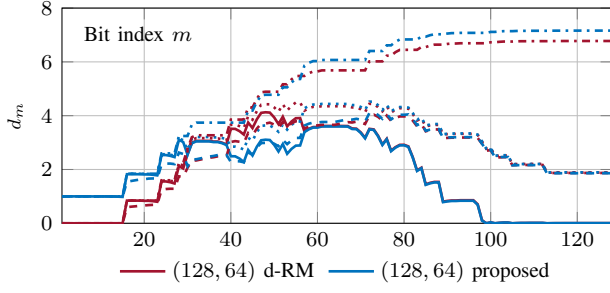


Fig. 1. d_m vs. m at $E_b/N_0 = 0.5$ dB for (128, 64) codes (dash-dotted: upper bound (5b), solid: lower bound (5a), dotted: d_m via simulation, dashed: $\mathbb{E}[\log_2 |S_{0.94}^{(m)}|]$ via simulation).

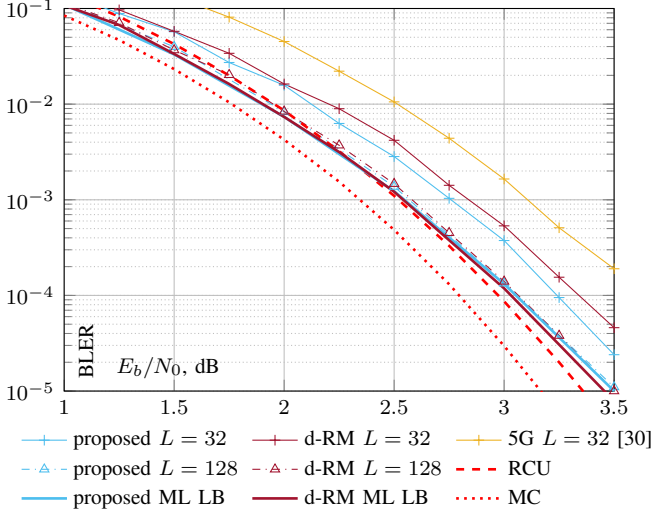


Fig. 2. BLER vs. SNR for (128, 64) codes.

Next, consider moderate-length codes, e.g., (512, 256) codes, which are more challenging to design if the decoders are restricted to be of low- to moderate-complexity, i.e., $L \leq 1024$ [4, Sec. 5.2] [31]. Fig. 3 provides the bounds (5a) for d-RM codes and three novel designs. The peak of the lower bound corresponding to the d-RM code gets close to 25 and recall that this quantity is related to the logarithm of the required list size. This explains why an SCL decoder needs very large list sizes for a good performance when used for the RM(4, 9) (or a d-RM(4, 9)) code [32]. At the other extreme, the lower bound is provided for the construction based on the polarization weight (PW) method with $\beta = 2^{1/4}$ [33], which is more suitable for SCL decoding with small list sizes. The idea behind the designs is similar to the length-128 case: we start from the information positions of an RM code, modify the positions to lower the peak value and keep the curve flat so that there is enough entropy kept on the list to make use of reliable frozen positions for a good performance. To this end, we also introduced u_1 as information bit in all three designs. This would harm the performance if the list size is very small, e.g., $L \leq 4$. In modifying the designs, we used the information positions from the PW construction. The information positions for the designs are provided in the appendix.

Fig. 4 compares the performance of three designs under different list sizes. Code-1 requires the largest list size to get closer to its ML performance. When a large list size is adopted,

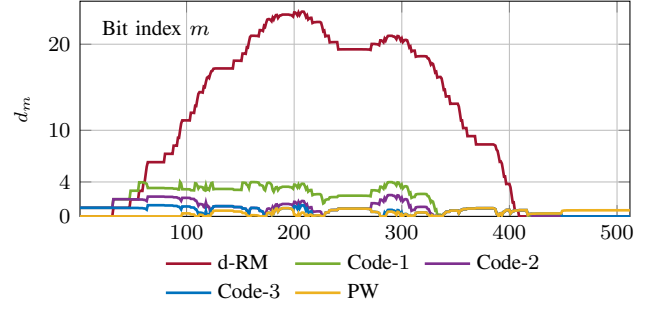


Fig. 3. Lower bound (5a) on d_m at $E_b/N_0 = 0.5$ dB for (512, 256) codes.

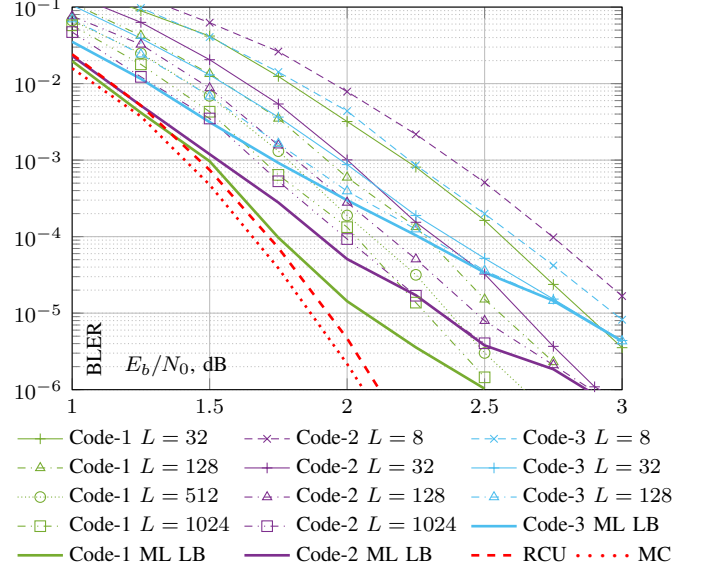


Fig. 4. BLER vs. SNR for (512, 256) codes.

e.g., $L \in \{512, 1024\}$, it performs within 0.4 dB of the RCU bound at block error rates around 10^{-6} , outperforming the non-binary LDPC code defined over \mathbb{F}_{256} which has a higher decoding complexity [31]. Nevertheless, even with $L = 1024$, there is a non-negligible gap to the ML lower bound at block error rates above 10^{-6} . Code-2 is competitive for a wide range of list sizes, i.e., $L \in \{8, 32, 128, 1024\}$. In particular, it performs within 0.75 dB from the RCU bound down to the block error rate of 10^{-6} under SCL decoding with $L = 32$, outperforming the 5G design [30] by around 0.2 dB under the same list size (see Fig. 5). When an even smaller list size considered, e.g., $L = 8$, then Code-2 and the 5G design are indistinguishable while Code-3, which is expected to perform well under small list sizes (see Fig. 3), outperforms them by around 0.15 dB at all error rates shown. With a relatively small list size, e.g., $L = 32$, Code-3 reaches to its ML performance at a block error rate of 10^{-5} or less.

B. The Binary Erasure Channel

To understand the accuracy of the analysis and approximations presented in Sections III and IV, we simulated the SCI decoder with consolidation. The results of these simulations are realizations of the random process D_1, \dots, D_N .

One weakness of these bounds is that the channel variation (e.g., in the number of erasures) significantly increases the

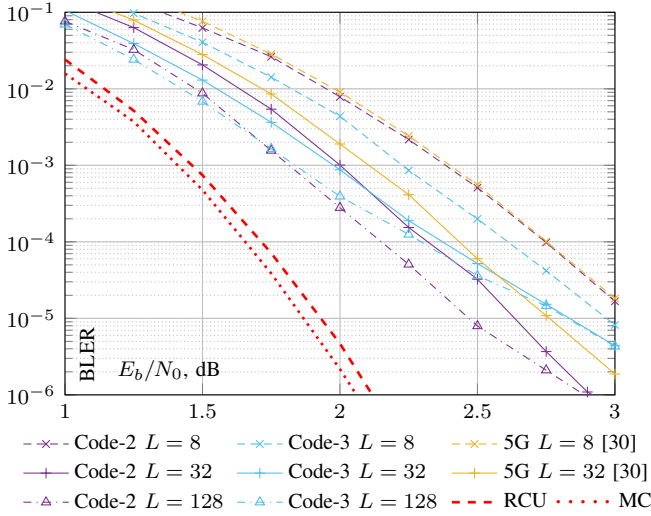


Fig. 5. BLER vs. SNR for (512, 256) 5G codes compared to new designs.

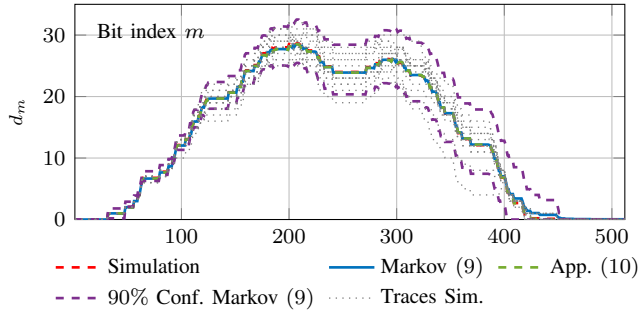


Fig. 6. d_m vs. m for randomly permuted 246 erasures.

variation in D_1^N . To highlight the similarity between the theory and simulation, we use a fixed-weight BEC that chooses a random pattern with exactly $\text{round}(N\epsilon)$ erasures. To motivate this, note that density evolution naturally captures the typical behavior of the analyzed system [26]. Fig. 6 shows simulation results for realizations of D_1^N and compares these with their average and the theoretical predictions (9) and (10). These results show that, for a random (512, 256) d-RM code, the simulation mean is close to the analysis. The 15 random simulation traces lie largely within the 90% confidence range of the Markov chain analysis.

Next, a *d-RM ensemble sequence* is introduced as the sequence of rate- $1/2$ d-RM ensembles. The ℓ -th ensemble in the sequence is $\mathcal{C}(\ell, 2\ell + 1)$. We study how the subspace dimension behaves as the block length increases. Note that as the block length changes, a random instance from the corresponding ensemble is picked for the simulations. The numerical results are quite similar for different instances chosen randomly. Let $w \triangleq \frac{m}{N}$, $m \in [N]$, be the normalized decoding stage. Fig. 7 provides the normalized dimension $\frac{1}{N}d_{wN}$ as a function of w for the samples of d-RM ensemble sequence with different block lengths, from $N = 2^9$ up to $N = 2^{31}$. The match between the approximation (10) and the simulation up to $N = 2^{13}$ shows the accuracy of the analysis and we believe that the results for larger block lengths are also accurate. The asymptotic behavior of $\frac{1}{N}d_{wN}$ gives the asymptotic decoding complexity of an ML decoder

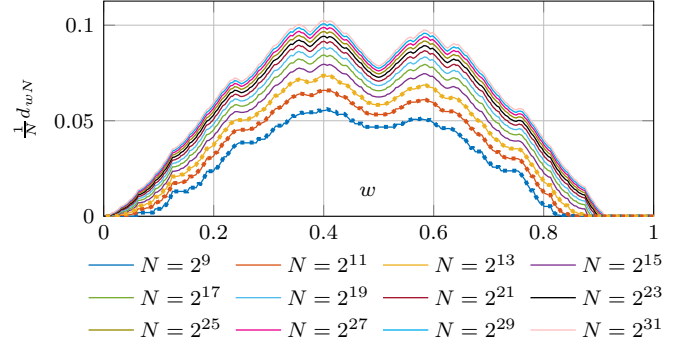


Fig. 7. $\frac{1}{N}d_{wN}$ vs. w (solid: using (10) with an erasure probability $\epsilon = 0.48$, dashed: simulations for the fixed-weight BEC with $\text{round}(N\epsilon)$ erasures) for instances from d-RM code ensembles $\mathcal{C}(\ell, 2\ell + 1)$, $\ell \in \{4, 5, \dots, 15\}$.

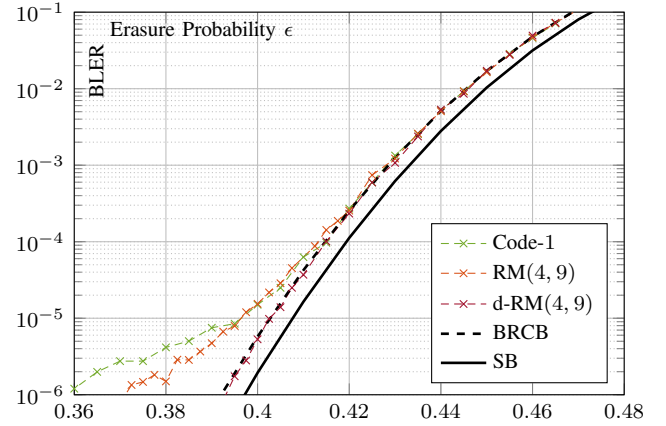


Fig. 8. BLER vs. ϵ for (512, 256) codes.

implemented via an SCI decoder. This provides insight into the asymptotic decoding complexity of RM codes to achieve the capacity over the BEC [34] for two reasons: first, RM code is a member of the ensemble, and second, the simulation results look very similar for RM codes as well up to $N = 2^{13}$. Other decoding algorithms might give improvements on the complexity, but we are not aware of a lower-complexity ML decoder than SCI decoding for RM codes. Fig. 7 shows that the convergence seems to be rather slow for the defined sequence. Interesting directions include understanding what happens to $\frac{1}{N}d_{wN}$ as $N \rightarrow \infty$ analytically and trying to define code sequences where $\max_w \frac{1}{N}d_{wN}$ is significantly better than that of d-RM codes, but still perform competitively.

Finally, Fig. 8 compares the ML decoding performance of Code-1 designed in Section V-A to that of the RM(4, 9) and a random instance from $\mathcal{C}(4, 9)$ by using SCI decoder. We declare an error whenever the linear system corresponding to the channel output does not provide a unique solution. The code performs as well as the RM(4, 9) code for frame error rates equal to 10^{-5} or higher with much lower average subspace dimension during decoding as illustrated in Fig. 9. Thus, we can match random code performance (like d-RM) down to the block error rate of 10^{-4} while performing well with smaller number of inactivations (i.e., shorter list sizes). For block error rate of 10^{-5} or less, it experiences more severe error floor compared to the RM(4, 9) code. The Singleton bound (SB) [35] and the Berlekamp's random coding bound

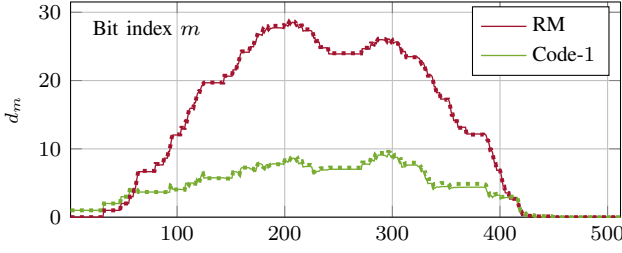


Fig. 9. d_m vs. m for Code-1 compared to the RM code (solid: using (10) with an erasure probability of $\epsilon = 0.48$, dashed: simulations for the fixed-weight BEC with 246 erasures).

(BRCB) [36] are provided as reference.

VI. CONCLUSION

In this paper, we consider the theoretical question “What list size suffices to achieve ML decoding performance under an SCL decoder?”. The results identify information-theoretic quantities associated with the required list size and also lead to a natural approximation that can be computed efficiently even for very long codes. The logarithm of the random required list size concentrates around the mean. A simple recursive approximation of this mean is provided for the BEC.

Simulation results show that this approximation captures the dynamics of the required list size at each stage of decoding on the BEC. For general BMS channels, e.g., biAWGNC, the analysis identified the key quantity d_m as a proxy for the uncertainty in the SCL decoding. The analysis suggested codes with improved performance under SCL decoding with various practical list sizes, e.g., $L \in \{8, 32, 128\}$ for short- to moderate-length codes. Future work should devise a constructive algorithm which take into account the introduced quantities to design good codes for SCL decoding with practical list sizes for wider range of block lengths, e.g., for $N \leq 2048$.

ACKNOWLEDGEMENT

The authors thank Gerhard Kramer (TUM) for comments improving the presentation.

APPENDIX

A. The Designs for (512, 256) Case

Let \mathcal{A}_{PW} denote the set of information positions of the (512, 256) polar code designed according to PW with $\beta = 2^{1/4}$ [33]. The sets \mathcal{A}_1 , \mathcal{A}_2 and \mathcal{A}_3 corresponding to Code-1, Code-2 and Code-3, respectively, are given as follows:

$$\begin{aligned} \mathcal{A}_3 &= (\mathcal{A}_{PW} \setminus \{449, 450, 451, 453, 457, 465, 481\}) \\ &\quad \cup \{1, 64, 118, 122, 159, 200, 284\}, \\ \mathcal{A}_2 &= (\mathcal{A}_3 \setminus \{122, 421, 425, 433\}) \cup \{32, 174, 272, 280\}, \\ \mathcal{A}_1 &= (\mathcal{A}_2 \setminus \{64, 96, 125, 180, 418, 419\}) \\ &\quad \cup \{48, 56, 94, 108, 122, 152\}. \end{aligned}$$

For all codes, each frozen bit is set to a random linear combination of preceding information bit(s). The performance curves will also be available on [30].

REFERENCES

- [1] M. C. Coşkun and H. D. Pfister, “Bounds on the list size of successive cancellation list decoding,” in *2020 Int. Conf. on Signal Process. and Commun. (SPCOM)*, 2020, pp. 1–5.
- [2] E. Arkan, “Channel polarization: A method for constructing capacity-achieving codes for symmetric binary-input memoryless channels,” *IEEE Trans. Inf. Theory*, vol. 55, no. 7, pp. 3051–3073, Jul. 2009.
- [3] I. Tal and A. Vardy, “List decoding of polar codes,” *IEEE Trans. Inf. Theory*, vol. 61, no. 5, pp. 2213–2226, May 2015.
- [4] M. C. Coşkun, G. Durisi, T. Jerkovits, G. Liva, W. Ryan, B. Stein, and F. Steiner, “Efficient error-correcting codes in the short blocklength regime,” *Elsevier Phys. Commun.*, vol. 34, pp. 66–79, Jun. 2019.
- [5] “LS on channel coding,” 3GPP TSG RAN WG1 Meeting, R1-1715317, Prague, Czech Republic, Tech. Rep. 90, Aug. 2017.
- [6] P. Trifonov and V. Miloslavskaya, “Polar subcodes,” *IEEE J. Sel. Areas Commun.*, vol. 34, no. 2, pp. 254–266, Feb. 2016.
- [7] P. Trifonov and G. Trofimuk, “A randomized construction of polar subcodes,” in *Proc. IEEE Int. Symp. Inf. Theory*, 2017, pp. 1863–1867.
- [8] P. Yuan, T. Prinz, G. Böcherer, O. İşcan, R. Böhnke, and W. Xu, “Polar code construction for list decoding,” in *Proc. 11th Int. ITG Conf. on Syst., Commun. and Coding (SCC)*, Feb. 2019, pp. 125–130.
- [9] A. Elkelesh, M. Ebada, S. Cammerer, and S. ten Brink, “Decoder-tailored polar code design using the genetic algorithm,” *IEEE Trans. Commun.*, vol. 67, no. 7, pp. 4521–4534, 2019.
- [10] A. Fazeli, A. Vardy, and H. Yao, “Convolutional decoding of polar codes,” in *IEEE Int. Symp. on Inf. Theory*, 2019, pp. 1397–1401.
- [11] M. Rowshan and E. Viterbo, “How to modify polar codes for list decoding,” in *IEEE Int. Symp. Inf. Theory*, Jul. 2019, pp. 1772–1776.
- [12] E. Arkan, “From sequential decoding to channel polarization and back again,” *CoRR*, vol. abs/1908.09594, 2019. [Online]. Available: <http://arxiv.org/abs/1908.09594>
- [13] V. Miloslavskaya and B. Vucetic, “Design of short polar codes for SCL decoding,” *IEEE Trans. Commun.*, vol. 68, no. 11, pp. 6657–6668, 2020.
- [14] I. Reed, “A class of multiple-error-correcting codes and the decoding scheme,” *Trans. IRE Prof. Group on Inf. Theory*, vol. 4, no. 4, pp. 38–49, Sep. 1954.
- [15] D. E. Muller, “Application of boolean algebra to switching circuit design and to error detection,” *Trans. IRE Prof. Group on Electronic Computers*, vol. EC-3, no. 3, pp. 6–12, Sep. 1954.
- [16] M. G. Luby, M. Mitzenmacher, M. A. Shokrollahi, and D. A. Spielman, “Analysis of low density codes and improved designs using irregular graphs,” in *Proc. ACM Symp. on Theory of Computing*, ser. STOC ’98. New York, NY, USA: Association for Computing Machinery, 1998, p. 249–258. [Online]. Available: <https://doi.org/10.1145/276698.276756>
- [17] T. J. Richardson and R. L. Urbanke, “The capacity of low-density parity-check codes under message-passing decoding,” *IEEE Trans. Inf. Theory*, vol. 47, no. 2, pp. 599–618, 2001.
- [18] N. Stolte, “Rekursive Codes mit der Plotkin-Konstruktion und ihre Decodierung,” Ph.D. dissertation, TU Darmstadt, 2002.
- [19] I. Dumer and K. Shabunov, “Near-optimum decoding for subcodes of Reed-Muller codes,” in *Proc. IEEE Int. Symp. Inf. Theory*, 2001, p. 329.
- [20] J. Neu, “Quantized polar code decoders: Analysis and design,” *CoRR*, vol. abs/1902.10395, 2019. [Online]. Available: <http://arxiv.org/abs/1902.10395>
- [21] M. C. Coşkun, J. Neu, and H. D. Pfister, “Successive cancellation inactivation decoding for modified Reed-Muller and eBCH codes,” in *IEEE Int. Symp. Inf. Theory*, 2020, pp. 437–442.
- [22] A. Shokrollahi, “Raptor codes,” *IEEE Trans. Inf. Theory*, vol. 52, no. 6, pp. 2551–2567, Jun. 2006.
- [23] C. Measson, A. Montanari, and R. Urbanke, “Maxwell construction: The hidden bridge between iterative and maximum a posteriori decoding,” *IEEE Trans. Inf. Theory*, vol. 54, no. 12, pp. 5277–5307, Dec. 2008.
- [24] A. Eslami and H. Pishro-Nik, “On bit error rate performance of polar codes in finite regime,” in *Proc. Allerton Conf. on Commun., Control, and Comput.*, Sep. 2010, pp. 188–194.
- [25] M. Mitzenmacher and E. Upfal, *Probability and Computing: Randomized Algorithms and Probabilistic Analysis*. USA: Cambridge University Press, 2005.
- [26] T. Richardson and R. Urbanke, *Modern Coding Theory*. New York, NY, USA: Cambridge University Press, 2008.
- [27] H. Yao, A. Fazeli, and A. Vardy, “List decoding of Arkan’s PAC codes,” in *Proc. IEEE Int. Symp. Inf. Theory*, 2020, pp. 443–448.
- [28] M. Rowshan, A. Burg, and E. Viterbo, “Polarization-adjusted convolutional (PAC) codes: Sequential decoding vs list decoding,” *IEEE Trans. Veh. Technol.*, vol. 70, no. 2, pp. 1434–1447, 2021.

- [29] Y. Polyanskiy, V. Poor, and S. Verdù, "Channel coding rate in the finite blocklength regime," *IEEE Trans. Inf. Theory*, vol. 56, no. 5, pp. 2307–235, May 2010.
- [30] G. Liva and F. Steiner, "pretty-good-codes.org: Online library of good channel codes," <http://pretty-good-codes.org>, Mar. 2021.
- [31] O. İşcan, D. Lentner, and W. Xu, "A comparison of channel coding schemes for 5G short message transmission," in *IEEE Global Commun. Conf. Workshops*, 2016, pp. 1–6.
- [32] M. Mondelli, S. H. Hassani, and R. L. Urbanke, "From polar to Reed-Muller codes: A technique to improve the finite-length performance," *IEEE Trans. Commun.*, vol. 62, no. 9, pp. 3084–3091, Sep. 2014.
- [33] G. He, J. Belfiore, I. Land, G. Yang, X. Liu, Y. Chen, R. Li, J. Wang, Y. Ge, R. Zhang, and W. Tong, "Beta-expansion: A theoretical framework for fast and recursive construction of polar codes," in *IEEE Global Commun. Conf.*, 2017, pp. 1–6.
- [34] S. Kudekar, S. Kumar, M. Mondelli, H. D. Pfister, E. Şaşıoğlu, and R. L. Urbanke, "Reed-Muller codes achieve capacity on erasure channels," *IEEE Trans. Inf. Theory*, vol. 63, no. 7, pp. 4298–4316, Jul. 2017.
- [35] R. Singleton, "Maximum distance q-ary codes," *IEEE Trans. Inf. Theory*, vol. 10, no. 2, pp. 116–118, Apr. 1964.
- [36] E. R. Berlekamp, "The technology of error-correcting codes," *Proc. IEEE*, vol. 68, no. 5, pp. 564–593, May 1980.